Non-Linear Dynamics and Chaos: The PN Junction

Nico Deshler*
Physics Department, University of California Berkeley.
(Dated: May 14, 2021)

This work is an exploration in non-linear dynamics and chaos. Our system of focus is the PN junction - a driven oscillatory circuit containing a semiconducting diode with a non-linear response. Of principal interest is the relationship between the chaotic parameters and the dynamical variables. For the PN junction these are, respectively, the amplitude of a tunable voltage source and the electrical current of the circuit. The dynamics of this system are analyzed in simulation. In particular, we numerically integrate the dynamical equations of the circuit and explore the periodicity of state space orbits. Bifurcation diagrams plotted over a progression of the chaotic parameter demonstrate sequential period doubling and cycling between chaotic and stable bands. Informed by these visualizations, we identify a strange attractor for the circuit. We also explore delay time embeddings of the current in two and three dimensions. Finally, we compute the largest Lyapunov exponent for different values of the chaotic parameter.

Key Terms: PN Junction, State Space, Lyapunov Exponent, Bifurcation Diagram, Return Map, Feigenbaum Constant

I. INTRODUCTION

Non-linear dynamics is the study of complex systems whose temporal evolution is governed by non-linear equations. These equations are often difficult to solve analytically, leaving scientists to appeal to numerical methods for understanding them. The subclass of dynamical systems that are described by solvable differential equations have been deeply illuminating. However, nature often challenges us with dynamical systems that elude all efforts to describe them in closed form. Even the dynamics of the simple pendulum is in truth non-linear. Only after making a small-angle approximation can one recover the differential equation of a harmonic oscillator.

'Chaos' is an emergent phenomena of non-linear dynamics. Here the term refers to dynamical systems characterized by three features: 1) Their evolution is aperiodic (trajectories in state space do not repeat themselves), 2) they are highly sensitive to changes in initial conditions, 3) they tend to evolve towards certain bounded regions of state space called attractors. It is important to emphasize that chaotic systems are not stochastic - on the contrary they follow deterministic rules. However, under these rules, it quickly becomes difficult to predict the evolution of a chaotic system with any precision since small uncertainties in the initial conditions grow exponentially quickly.

The techniques for studying non-linear dynamics have made headway in virtually every scientific field. In meteorology, the Lorenz equations proposed for modelling atmospheric convection gave birth to modern chaos theory [1]. In biology, the transport of gene mutations across generations was found to follow the Huxley-Fisher nonlinear diffusion equation [2]. In environmental science, the interplay of natural resource extraction and population growth has been successfully modelled and analyzed as a non-linear system [3]. Interesting behavior has been uncovered in all of these non-linear models using the techniques employed in this work.

In this study, we investigate a continuous-time nonlinear system called the PN junction circuit. The current oscillations in this circuit are rich in chaotic behavior and lie at the focus of the study. Numerical methods are used to evaluate state space trajectories, generate bifurcation diagrams, plot time delay embeddings, and compute Lyapunov constants.

II. THEORY

A. Preliminaries

1. State Space

A dynamical system is expressed in terms of its dynamical variables. These are the time-dependent quantities apparent in the system's equations of motion (e.g. the x, y, and z coordinates of a moving body and the components of its momentum p_x, p_y, p_z). The term 'motion' is used here as a synonym for 'change'. The state $\mathbf{x}$ of a system is simply a list of all dynamical variables at a given instant in time:

$$\mathbf{x} = [x^{[1]}, x^{[2]}, ..., x^{[m]}]$$

The state space (or phase space) is defined by a set of all states available to the system $\mathbb{R}^m$ and an evolution operator $\phi : \mathbb{R}^m \to \mathbb{R}^m$ that propagates a state in time. The evolution operator must satisfy the property that

$$\phi_t(\phi_s(\mathbf{x})) = \phi_{t+s}(\mathbf{x})$$

* nico.deshler@berkeley.edu

A state space can also be ordained with a probability measure over all states. Though discussion of this measure is beyond the scope of our work.

2. Flow for Continuous-Time Systems

For a continuous-time system, the evolution operator ϕ can be understood by considering a vector field $\mathbf{F}(\mathbf{x})$ over the state space. The direction of this vector field at any point represents the instantaneous time-evolution of the system. Consequently, the components of $\mathbf{F}$ are the time derivatives of the state variables.

$$\begin{aligned} F_1 &= \dot{x}^{[1]} = f_1(\mathbf{x}) \\ F_2 &= \dot{x}^{[2]} = f_2(\mathbf{x}) \\ &\vdots \\ F_m &= \dot{x}^{[m]} = f_m(\mathbf{x}) \end{aligned}$$

Note that each of these equations are autonomous by requirement - they have no explicit time-dependence. This is important because it allows us to express the evolution of the system in terms of its state alone. We can express the vector field compactly as,

$$\mathbf{F}(\mathbf{x}) = \dot{\mathbf{x}}|_{\mathbf{x}}$$

The evolution operator $\phi : \mathbf{x}(0) \to \mathbf{x}(\tau)$ takes a point in state space and maps it to another point in state space that represents the system at a later time τ. Formally,

$$\phi_\tau(\mathbf{x}) = \int_0^\tau \mathbf{F}(\mathbf{y}(t))dt \quad , \quad \mathbf{y}(0) = \mathbf{x} \tag{1}$$

The locus of points generated by applying the evolution operator over infinitesimal time intervals forms a trajectory through state space. Intuitively, this trajectory follows the vector field. The flow diagram over state space shown in Figure 1 helps illustrate this idea.

3. Lyapunov Exponents

The central tenet of chaotic systems is that small perturbations to initial conditions produce quickly diverging trajectories in state space. It is possible to characterize the rate of this divergence with Lyapunov exponents.

Consider two close initial states $\mathbf{x_0}$ and $\mathbf{x_0}+\epsilon$. Our goal will be to quantify the rate at which the perturbation ϵ grows. Taylor expanding the perturbed initial state gives,

$$\phi_t(\mathbf{x}_0 + \epsilon) = \phi(\mathbf{x}_0) + J(t)\epsilon + O(|\epsilon|^2)$$

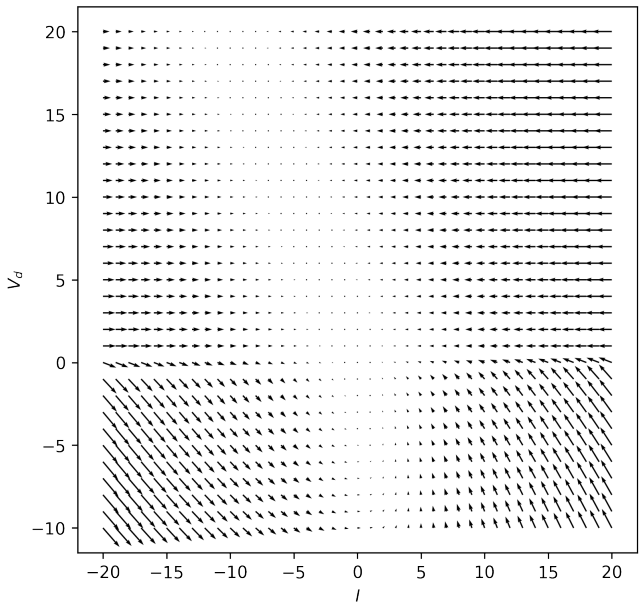

FIG. 1: A computed flow over a the state space of the PN junction. The two state variables of interest are the current I and the voltage drop over the diode V_d. The flow vectors are computed using Equation 8. The bounds of the x-axis span simulated saturation current for the diode. For $V_d > 0$ the system appears to be convergent as all vector field directions point inward towards a region of fixed points.For Vd ¡0 the flow cycles back into the convergent region. Hence the dynamics for the portion of state space shown are convergent. Indeed the vector field was rendered with a small choice of the chaotic parameter. Higher values would generate a more aggressive flow field.

where $J(t)$ is the Jacobian matrix given by the linearization of ϕ_t about $\mathbf{x_0}$,

$$J(t) = \frac{\partial \phi_t(\mathbf{x}_0)}{\partial \mathbf{x}_0} = \frac{\partial \mathbf{x}(t)}{\partial \mathbf{x}(0)} \tag{2}$$

$$J_{ij}(t) = \frac{\partial \mathbf{x}_i(t)}{\partial \mathbf{x}_j(0)} \tag{3}$$

We see that the perturbation ϵ gets transformed as $J(t)\epsilon$. The eigenvalues of $J(t)$ express the rate of divergence between nearby trajectories along orthogonal directions in R^m. The determinant of $J(t)$ describes the local contraction/expansion of state space (dissipation). Since the determinant is the sum of the eigenvalues, a positive eigenvalue sum indicates that the distance between nearby trajectories grows exponentially quickly. If their sum is negative, then nearby trajectories converge exponentially quickly. Formally, the limit of these eigenvalues are the Lyapunov exponents shown in Equation 4.

$$\lambda_k = \lim_{t\to\infty} \frac{1}{t} \log(\mathrm{k}^{th} \text{ eigenvalue of } J(t)) \tag{4}$$

This definition of the Lyapunov exponents is analytically useful in that it is written in terms of computable quantities [4]. However the interpretation of the limit here is not obvious. An more easily interpreted formulation of the Lyapunov exponents is,

$$\lim_{t\to\infty}\lim_{|\epsilon_0|\to 0}\frac{1}{t}\frac{|\epsilon(t)|}{|\epsilon_0|} \tag{5}$$

where $\epsilon(t) = J(t)\epsilon$ is the perturbation at a later time t. The interpretation of the limits is now more clear. We wish to evaluate how an infinitesimal perturbation in the initial conditions compares to itself looking ahead far into the future.

4. Time of Unpredictability

Suppose the state of a chaotic system is experimentally measured at time t_0 to a precision ϵ. One question we may ask is 'how long must we wait until nothing is known about the state?' This question motivates an alternative information perspective of chaos that is particularly pertinent to numerical simulation of continuous-time dynamical systems. .

Let us first address this question. From an information perspective, the sum of the positive Lyapunov exponents can be thought of as the rate of information loss h_μ about the state. After all, we saw from derivation of Equation 4 that nearby state space trajectories diverge along the directions of the eigenvectors of $J(t)$ corresponding to the positive Lyapunov exponents. Suppose the measurement precision ϵ is one part in 2^n. The number of bits required to express a measurement is the information I known about the system $I(\epsilon) = -\log_2\epsilon$. The rate of information loss is $h_\mu[\frac{\text{bits}}{\text{sec}}]$. Therefore the time to unpredictability of the system becomes

$$\tau_u = \frac{I(\epsilon)}{\mu_h} = \frac{-\log_2\epsilon}{\mu_h} = \frac{n}{\mu_h}$$

Many numerical ODE solvers like the ones used in this work simulate the dynamics of the PN junction instantiate a small discrete time step with which to propagate the dynamical equations. If this time step is greater than the time to unpredictability, then the validity of the integration is dubious.

B. The PN Junction

The PN junction circuit shown in Figure 2. We consider two dynamical state variables: the current through the circuit I and the voltage drop across the diode V_d. Thus the state is defined as $\mathbf{x} = [I, V_d]$. The exploded view of the circuit diagram demonstrates how the diode can be modelled a current source I_d and a capacitor C in parallel. Both of these elements have a non-linear dependence on V_d given by equations 6 and 7 respectively.

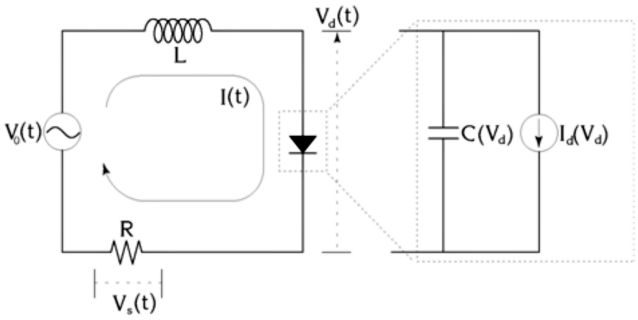

FIG. 2: A circuit diagram of the PN junction. Without the diode, this circuit is the well-known driven damped oscillator RL circuit which has analytic solutions. The non-linearity introduced by the diode naturally brings forth chaotic behavior in this system.

$$I_d(V_d) = I_{sat}(\exp(\frac{qV_d}{kT}) - 1) \tag{6}$$

$$C(V_d) = \begin{cases} C_0\exp(\frac{qV_d}{kT}) & V_d > 0 \\ \frac{C_0}{\sqrt{1-\frac{qV_d}{kT}}} & V_d < 0 \end{cases} \tag{7}$$

Here I_{sat} is the saturation current of the diode, q is the charge of an electron, and kT is the Boltzmann constant times the temperature. The system is driven by an oscillating voltage source V_o

$$\begin{aligned} V_o(t) &= V_0 sin(\omega t) \\ &= V_0 sin(\theta) \end{aligned}$$

where, to eliminate the explicit time dependence, we have introduced a new state variable $\theta = \omega t$. Since θ is now another dynamical quantity it is included in our state vector $\mathbf{x} = [V_d, I, \theta]$. Applying Kirchoff's Law to the circuit and using the equations for a resistor, a capacitor, and an inductor [see Appendix Section A for a complete derivation] one finds the dynamical equations 8a, 8b, 8c for the circuit.

$$\dot{V}_d = \frac{I - I_d(V_d)}{C(V_d)} \tag{8a}$$

$$\dot{I} = \frac{V_0\sin(\theta) - V_d - IR}{L} \tag{8b}$$

$$\dot{\theta} = \omega \tag{8c}$$

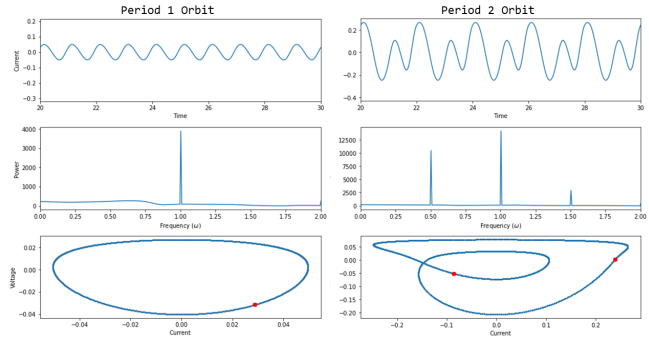

FIG. 3: Circuit current, frequency spectrum, and phase space trajectories for period 1 and 2 orbits. The driving amplitudes were set to 0.019 and 0.13 respectively.

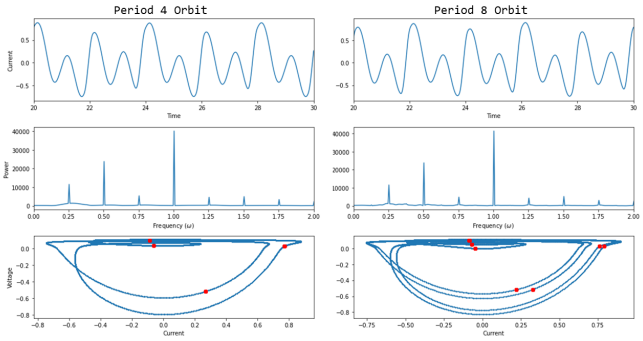

FIG. 4: Circuit current, frequency spectrum, and phase space trajectories for period 4 and 8 orbits. The driving amplitudes were set to 0.405 and 0.4137 respectively.

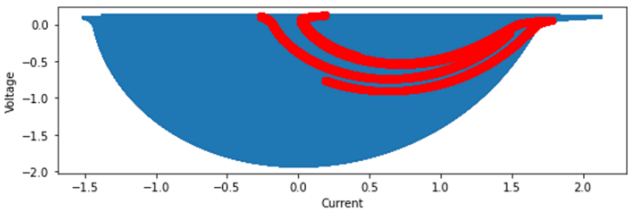

FIG. 5: The attractor of the PN junction (blue region) found by tracing an aperiodic chaotic trajectory over 60 million timesteps. 60 thousand cycles of the return map are plotted in red demonstrating interesting structure.

III. NUMERICAL METHODS AND ANALYSIS

Several analytical methods have been devised for characterizing chaos. Most provide a geometric representation of the system dynamics. In this work we simulate the PN junction computationally and investigate how the drive amplitude V_0 affects the evolution of the state. The *Pynamical* package in Python package offers several visualizations tools for non-linear dynamics that we utilize in the following sections.

A. State Space Trajectories and Spectral Analysis

Numerical integration of the dynamical equations allows us to trace trajectories through the state space. When the system is not in a chaotic regime, these trajectories settle into closed loops that befit the name 'orbits'. The PN junction simulation was configured to evolve for 60 cycles of the sinusoidal drive before observation to avoid capturing transient dynamics.

Figures 3 and 4 show transitions in the periodicity of stable state space trajectories for different driving amplitudes. A time series of the current and its Fourier Transformed are also shown to corroborate the periodic trajectories. As shown, there is a correspondence between the periodicity of the orbits, demarcated by the number of return map samples (red dots), and the number of prominent peaks that appear in the frequency spectrum of the current.

Inspecting the Period 4 and Period 8 orbits, it is clear that they share qualitative similarities. The narrow separation of the trajectory lines suggests that the drive voltage is near a bifurcation point. Identifying these precise bifurcation points is the topic of upcoming sections.

Figure 5 showcases a chaotic trajectory traced over tens of thousands of drive cycles. The dense population of state points elucidates a bounded blue region called an attractor. Initializations of the PN junction that fall in this region are guaranteed to remain in it no matter how the chaotic the resulting trajectory. Overlayed in red are the return map samples. This seemingly continuous locus of red points is representative of the aperiodicity of the chaotic trajectory. Had the trajectory been periodic, the number of red points would be finite. Complementing this notion, Figure 6 contains the return map itself. The return map shown is analogous to a Poincaré Map. Though instead of sampling the state at its intersection with a prescribed manifold in state space, the return map samples the trajectories at periodic time intervals. In the case of the PN junction it is natural to sample the current along the state trajectory at time intervals equal to the period of the sinusoidal drive.

B. Bifurcation Diagrams

Previously we showed that the periodicity of stable orbits could be observed from the state space trajectories and from the frequency spectrum of the dynamical variable. However, with these approaches alone it is difficult to register how the periodicity of the orbit varies with the chaotic parameter. Figure 7 presents a bifurcation diagram, which plots the return map samples against a scan

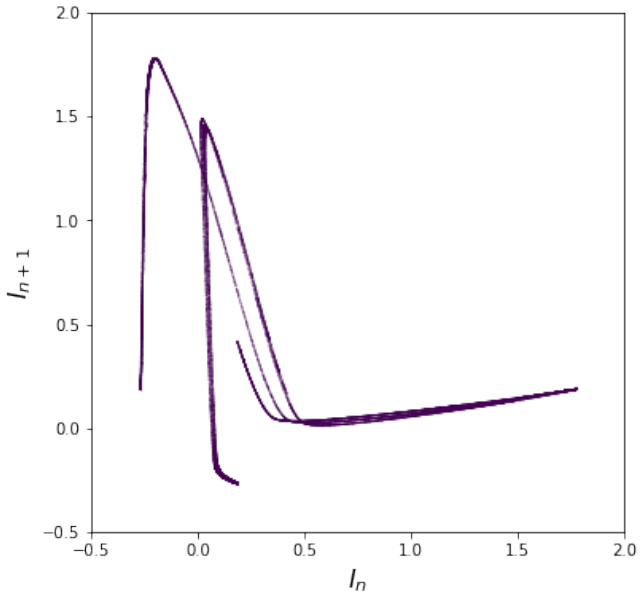

FIG. 6: An return map of a chaotic trajectory periodically sampled at rate ω. Note the topological similarity between the return map and the structure in Figure 5. Return maps reduce the dimensionality of the attractor in state space.

over a narrow region of the drive voltage. This region exhibits orbits with rapidly growing complexity. As the drive amplitude increases, the bifurcations become more frequent, tending towards chaos. Remarkably, a continuous chaotic parameter like the drive amplitude generates discrete behavior in the system dynamics.

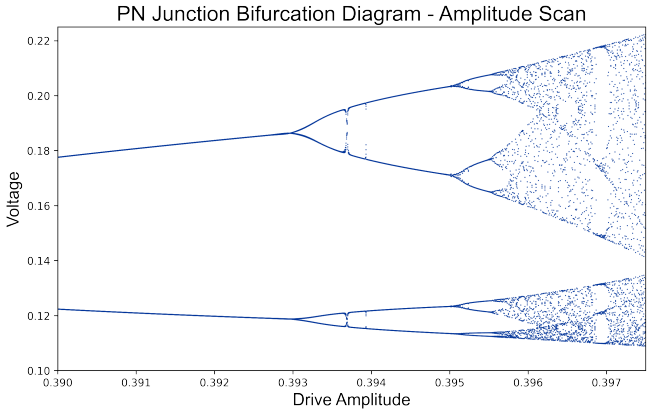

FIG. 7: A bifurcation diagram for the PN junction over a progression of drive amplitudes. The periodicity of the stable states increases in a fractal manner until reaching chaotic bands. Interspersed between these bands are regions of renewed periodicity.

Estimating the Feigenbaum Ratio

One common line of analysis stemming from bifurcation diagrams is calculating the Feigenbaum Ratio. This ratio relates the length of the intervals between bifurcations, which has been shown to converge. Let a_n the value of the chaotic parameter at the n^{th} bifurcation . The Feigenbaum ratio evaluated at a_n is defined as

$$\delta = \lim_{n\to\infty} \frac{a_{n-1} - a_{n-2}}{a_n - a_{n-1}}$$

As $n \to \infty$, this sequence tends towards a finite constant $\gamma \approx 4.669$ known as the Feigenbaum constant. Below we list the first five bifurcation points for the PN junction.

a_n	Amplitude	δ
a_1	0.094875	–
a_2	0.31817	–
a_3	0.3842	3.38172043
a_4	0.3931	7.41910112
a_5	0.3952	4.23809524
⋮	⋮	⋮

TABLE I: The first five bifurcation points for the PN junction and their corresponding Feigenbaum ratios are computed. With further samples of the bifurcation points this number will continue approaching the γ.

C. Delay Time Embedding

A Delay time embedding is another visualization tool for understanding state space trajectories and identifying chaotic attractors if only one of the dynamical variables is accessible. Here we showcase a delay time embedding of the PN junction current in a chaotic trajectory for two [Figure 8] and three dimensions [Figure 9].

D. Lyapunov Exponents for the PN Junction

Computing the Lyapunov exponents defined in equation 4 for continuous-time systems has been an area of active research [5], [6], [7]. While a multi-dimensional state spaces have several Lyapunov exponents, typically the largest Lyapunov exponent (LLE) provides a sufficient characterization of the chaos in the system. In this work we employ the *nolds* python package to compute the LLE from a time-series of the circuit current using the Rosenstein Algorithm [7].

IV. CONCLUSION

The PN junction provides a rich physical case study for investigating non-linear systems and chaos. In this

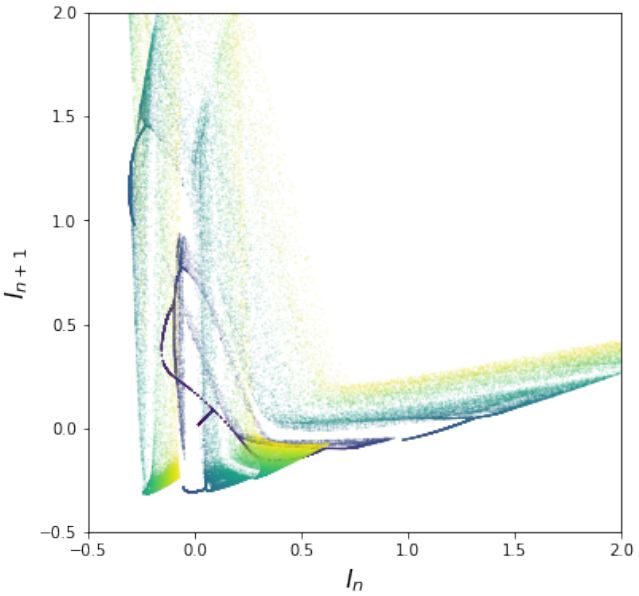

FIG. 8: A 2D embedding of the circuit current time-series. The current samples correspond to the chaotic trajectory through state space of the PN junction shown in 5. The distinct point colors distinguish between which cycle of the drive frequency they occur in.

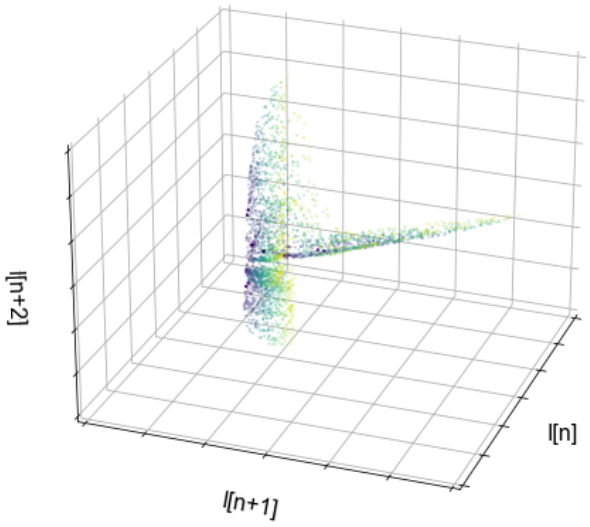

FIG. 9: A 3D embedding of the circuit current time-series.

work, we model the dynamics of the PN junction computationally. The fixed parameters for the dynamical simulations can be found in Appendix B. Our work begins with an overview of the mathematical formalisms for describing dynamical systems and the canonical methods for studying non-linear dynamics within this framework. Specifically, we present the state space, flow, and the Lyapunov exponents. The methods discussed include state space trajectories, bifurcation diagrams, delay time embeddings, and return maps. Taking the amplitude of the sinusoidal drive as our chaotic parameter, we proceed to analyze the PN junction using the aforementioned methods and report three principal findings. First, we characterize an for the PN junction. This attractor predominantly restricts the system to negative values of V_d. Second, we identify period doubling points and the onset of chaos for different intervals over the drive voltage. Third, we compute the largest Lyapunov exponent for different drive voltages and illustrate its approximate correspondence with the bifurcation plot.

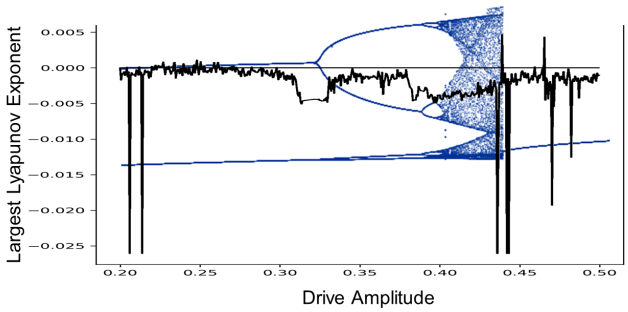

FIG. 10: Shown are the LLE overlayed onto the the bifurcation for a coincident range of the drive amplitude. As we can see the LLE is mostly negative for the regions where the bifurcation plot is stable. Near the bifurcation points the LLE exhibits a pronounced negative spike. This is explained by the merger of a stable and unstable fixed point. Around 0.45 Around 0. In contrast, the Lyap the bifurcation points we note dips in the tic regin

One intriguing aspect of chaos that was not addressed in this work is the fractal geometry of attractors. The correlation dimension of an attractor provides a dimensionality measure of the subspace of state space occupied by a chaotic dynamical system. The correlation dimension can be found by exploring time delay embeddings of increasing dimension and determining how the average number of points within a small hypercube scales. Such investigations present a compelling direction for future study.

ACKNOWLEDGMENTS

The author wishes to first acknowledge the amazing support of his colleague, Zachary Ross, for engaging in technical discussions of non-linear theory that proved deeply instructive. The author also wishes to acknowledge the support and enthusiasm provided by UC Berkeley's Physics 111B professors and Teaching Assistants amidst a trying academic year hampered by a global pandemic.

Appendix A: Deriving Dynamical Equations for PN Junction

The equations for the voltage across a resistor, a capacitor, and an inductor are given by

$$V_R = IR = \frac{dQ}{dt}$$
$$V_c = \frac{1}{C}Q$$
$$V_L = L\frac{dI}{dt} = L\frac{d^2Q}{dt^2}$$

Applying Kirchoff's law to the PN junction circuit gives us

$$V_o(t) = L\dot{I} + V_d + RI$$

We can reorder the terms to immediately determine Equation 8b

$$\dot{I} = \frac{V_0 \cos\theta - V_d - RI}{L}$$

Next, we solve for $\dot{V_d}$ by examining our model for the diode. We know from the voltage equation for a capacitor (listed above) that charge over the capacitor in the diode is $Q = CV_d$. Therefore, the current through the capacitor is $\dot{Q} = I_c = C\dot{V_d}$. By conservation of charge, the current entering the diode is given by the sum,

$$I = I_c + I_d(V_d)$$

Hence,

$$I = C\dot{V_d} + I_d V_d$$

$$\Rightarrow \dot{V_d} = \frac{I - I_d V_d}{C}$$

which is Equation 8a. Finally, since $\theta = \omega t$ by definition, $\dot{\theta} = \omega$ which is Equation 8c.

Appendix B: Simulation Parameters

The fixed simulation parameters of the PN junction are quoted here for reference.

The resistance and the inductance were chosen so that the resonance of the RL circuit was approximately of order one.

Appendix C: Drive Frequency ω as a Chaotic Parameter

Parameter	Variable Name	Value
Resistance	R	0.2
Inductance	L	1.0
Drive Frequency	ω	1.0
Diode Saturation Current	I_{sat}	20.0
Boltzmann Energy Normalization	kT	0.025
Initialized Diode Voltage	V_d	0.1
Initialized Circuit Current	V_d	0.1

TABLE II: Fixed simulation parameters and their values.

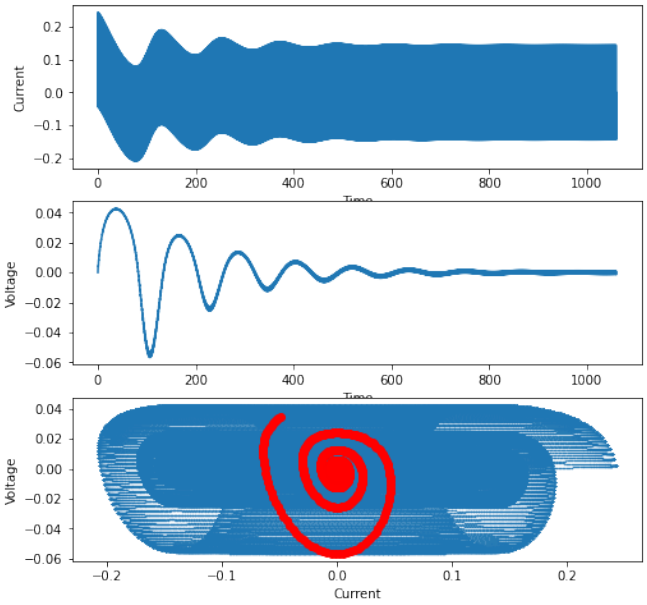

FIG. 11: Preliminary results of a spiral-tube strange attractor found in a chaotic trajectory incited by modulating the drive frequency. Here $\omega = 100$ and the drive amplitude were set to $V_0 = 15$. Interestingly, modulating the drive amplitude had the effect of rotating the tube about its short axis.

[1] E. N. Lorenz, Deterministic nonperiodic flow, Journal of Atmospheric Sciences **20**, 130 (1963).

[2] P. Broadbridge, B. Bradshaw-Hajek, G. Fulford, and

G. Aldis, Huxley and fisher equations for gene propagation: An exact solution, The ANZIAM Journal **44**, 11 (2002).

[3] S. D'Alessandro, Non-linear dynamics of population and natural resources: The emergence of different patterns of development, Ecological Economics **62**, 473 (2007).

[4] J. Theiler, Estimating fractal dimension, J. Opt. Soc. Am. A **7**, 1055 (1990).

[5] A. Dabrowski, Estimation of the largest lyapunov exponent-like (llel) stability measure parameter from the perturbation vector and its derivative dot product (part 2) experiment simulation, Nonlinear Dynamics **78**, 1601 (2014).

[6] J.-P. Eckmann, S. Kamphorst, D. Ruelle, and S. Ciliberto, Liapunov exponents from time series, Physical review. A **34**, 4971 (1987).

[7] M. T. Rosenstein, J. J. Collins, and C. J. De Luca, A practical method for calculating largest lyapunov exponents from small data sets, Physica D: Nonlinear Phenomena **65**, 117 (1993).

[8] E. Ott, *Chaos in Dynamical Systems*, 2nd ed. (Cambridge University Press, 2002).

[9] S. H. Strogatz, *Nonlinear dynamics and chaos with student solutions manual: With applications to physics, biology, chemistry, and engineering* (CRC press, 2018).